

EUROPEAN ORGANIZATION FOR NUCLEAR  
RESEARCH

CERN-EP/99-70  
DSF 15/99  
May 11, 1999

**A direct evaluation of the  $\Lambda_c^+$  absolute branching  
ratios: a new approach**

**P. Migliozi<sup>1</sup>**

CERN, Geneva, Switzerland

**G. D'Ambrosio, G. Miele, P. Santorelli**

Università Federico II and INFN, Napoli, Italy

**Abstract**

A novel method for a direct measurement of the exclusive  $\Lambda_c^+$  branching ratios is here described. The approach is based on the peculiar topology of the quasi-elastic charm neutrino-induced events on nucleons. The intrinsic potentiality of the method is thoroughly discussed using a *perfect detector*. As an application, the statistical accuracy reachable with existing data sample has been estimated. From a theoretical point of view, such measurement provides a better understanding of the baryonic b-decays.

*Submitted to Physics Letters B*

---

<sup>1</sup>Now also at the INFN, Sezione di Napoli, Italy

# 1 Introduction

There exists no direct measurement of  $BR(\Lambda_c^+ \rightarrow pK^-\pi^+)$ . However, using different assumptions and experimental data, two indirect determinations of the above branching ratio have been given [1, 2]. These two values are quite different, and thus it is likely that one of the procedures is incorrect.

Note that, since the channel  $\Lambda_c^+ \rightarrow pK^-\pi^+$  is used for normalisation, a change in its branching ratio will affect most of the  $\Lambda_c^+$  exclusive decay widths.

Here we propose a method, based on neutrino quasi-elastic charm production process, to directly measure the  $\Lambda_c^+$  branching ratios. This measurement, solving the above puzzle, will provide new insight on the underlying hadronic physics.

This letter has the following structure: in Section 2 we discuss the two different determinations of  $BR(\Lambda_c^+ \rightarrow pK^-\pi^+)$  and the physics impact of a direct measurement. In Section 3, the charm production in neutrino scattering is analysed by studying topology, kinematics and cross-sections of quasi-elastic processes and deep inelastic reactions, which are the main source of background. The evaluation of the accuracy achievable for these  $\Lambda_c^+$ -exclusive decay widths in neutrino scattering is performed in Section 4. In the last section, we give our conclusions.

## 2 Model dependent extraction of $BR(\Lambda_c^+ \rightarrow pK^-\pi^+)$

As stated above, two different methods to extract  $BR(\Lambda_c^+ \rightarrow pK^-\pi^+)$  from the experimental data have been proposed in literature [1, 2].

### Method A

The ARGUS [3] and CLEO [4] experiments have measured the quantity  $BR(\bar{B} \rightarrow \Lambda_c^+ X) \times BR(\Lambda_c^+ \rightarrow pK^-\pi^+)$ . Moreover, under the assumptions that  $\Gamma(\bar{B} \rightarrow \text{baryon } X)$  is dominated by  $\bar{B} \rightarrow \Lambda_c^+ X$ , CLEO [4] and ARGUS [5] have been able to determine the branching ratio  $BR(\bar{B} \rightarrow \Lambda_c^+ X)$ . Thus, combining these above measurements one obtains [1]

$$BR(\Lambda_c^+ \rightarrow pK^-\pi^+) = (4.14 \pm 0.91)\% . \quad (1)$$

It is worth pointing out, as emphasised in [2], that in order to derive  $BR(\bar{B} \rightarrow \Lambda_c^+ X)$

- i)  $\Xi_c$  and  $\Omega_c$  production in  $\bar{B}$ -decays,
- ii)  $\bar{B} \rightarrow D^* \bar{N} N X$  like decay channels

have been neglected.

### Method B

A different determination of  $BR(\Lambda_c^+ \rightarrow pK^-\pi^+)$  is based on the independent measurements of [6, 7]

$$\sigma(e^+e^- \rightarrow \Lambda_c^+ X) \times BR(\Lambda_c^+ \rightarrow pK^-\pi^+) , \quad (2)$$

and [8, 9]

$$\sigma(e^+e^- \rightarrow \Lambda_c^+ X) \times BR(\Lambda_c^+ \rightarrow \Lambda l^+ \nu_l). \quad (3)$$

Averaging over the results of the two experiments one obtains [1]

$$\begin{aligned} R &\equiv \frac{BR(\Lambda_c^+ \rightarrow pK^- \pi^+)}{BR(\Lambda_c^+ \rightarrow \Lambda l^+ \nu_l)} = \frac{\sigma(e^+e^- \rightarrow \Lambda_c^+ X) \times BR(\Lambda_c^+ \rightarrow pK^- \pi^+)}{\sigma(e^+e^- \rightarrow \Lambda_c^+ X) \times BR(\Lambda_c^+ \rightarrow \Lambda l^+ \nu_l)} \\ &= 2.40 \pm 0.43. \end{aligned} \quad (4)$$

Then the branching ratio for  $\Lambda_c^+ \rightarrow pK^- \pi^+$  can be obtained from the following relation

$$BR(\Lambda_c^+ \rightarrow pK^- \pi^+) = \frac{R \cdot f \cdot F}{1 + |V_{cd}/V_{cs}|^2} \Gamma(D^0 \rightarrow X l^+ \nu_l) \tau(\Lambda_c^+), \quad (5)$$

where

$$f \equiv \frac{BR(\Lambda_c^+ \rightarrow \Lambda l^+ \nu_l)}{BR(\Lambda_c^+ \rightarrow X_s l^+ \nu_l)}, \quad (6)$$

$$F \equiv \frac{\Gamma(\Lambda_c^+ \rightarrow X_s l^+ \nu_l)}{\Gamma(D^0 \rightarrow X_s l^+ \nu_l)}. \quad (7)$$

The ratio  $f$  is obviously  $<1$  since there are non-vanishing contributions to the leading  $X_s = \Lambda$  from  $\Sigma^\pm \pi^\mp$ , and  $n\bar{K}^0, pK^-$ , which however are phase space suppressed. The analogous fraction for the meson  $D$  has been measured by CLEO [10]

$$\frac{\Gamma(D \rightarrow (K + K^*) l^+ \nu_l)}{\Gamma(D \rightarrow X_s l^+ \nu_l)} = 0.89 \pm 0.12. \quad (8)$$

Thus one can reasonably expect  $f \simeq 0.9 \pm 0.1$ . In any case, experiments might measure  $f$  directly.

Theoretical estimates of  $F$  are based on Operator Product Expansion in the framework of the heavy quark effective theory [11], where the amplitudes for  $\Lambda_c^+ \rightarrow X_s l^+ \nu_l$  and  $D^0 \rightarrow X_s l^+ \nu_l$  are predicted to have the same leading terms, while the  $\mathcal{O}(1/m_c^2)$  corrections are found to be larger for  $\Lambda_c^+$ . As a result  $F = 1.3 \pm 0.2$  [11]. Thus, if one uses for  $R$  the value of Eq.(4) and [1] for

$$1 + |V_{cd}/V_{cs}|^2 = 1.05, \quad (9)$$

$$\Gamma(D^0 \rightarrow X l^+ \nu_l) = (0.163 \pm 0.006) \times 10^{12} \text{ s}^{-1}, \quad (10)$$

$$\tau(\Lambda_c^+) = (0.206 \pm 0.012) \times 10^{-12} \text{ s}, \quad (11)$$

we obtain from Eq.(5)

$$BR(\Lambda_c^+ \rightarrow pK^- \pi^+) = (7.7 \pm 1.5 \pm 2.3)\%. \quad (12)$$

Ref. [1] gives the weighted value of the two measurements  $BR(\Lambda_c^+ \rightarrow pK^- \pi^+) = (5.0 \pm 1.3)\%$ , where also the theoretical uncertainty is included. However, it is also stressed that this number is rather arbitrary. Indeed Ref. [2] advocates method  $\mathcal{B}$  suggesting that one should reanalyse the existing  $\bar{B} \rightarrow$  baryon sample to look for  $\bar{B} \rightarrow D^* \bar{N} N X$  decay channels. As a result, if this interpretation is correct, then:

$\sigma(10^{-39} \text{ cm}^2) \backslash \text{Model}$	F.R. [12]	S.L. [13]	A.K.K. [14, 15, 16]	A.G.Y.O. [17]	K. [18]
$\nu_\mu p \rightarrow \mu^- \Sigma_c^{++}$	0.02	0.9	0.8	0.1	0.3
$\nu_\mu p \rightarrow \mu^- \Sigma_c^{*++}$	0.06	1.6	1.0	0.06	-
$\nu_\mu n \rightarrow \mu^- \Lambda_c^+$	0.1	2.3	4.1	0.3	0.5
$\nu_\mu n \rightarrow \mu^- \Sigma_c^+$	0.01	0.5	-	0.06	0.15
$\nu_\mu n \rightarrow \mu^- \Sigma_c^{*+}$	0.03	0.8	-	0.03	-

Table 1: Predicted quasi-elastic charm production cross-section assuming a neutrino energy of 10  $GeV$ .

- i) heavy baryon tables would change;
- ii) measured charm counting in  $b$ -decay would decrease;
- iii)  $\bar{B} \rightarrow$  baryon decay models should be reanalysed.

### 3 Neutrino charm production

#### 3.1 Neutrino quasi-elastic charm processes

The simplest exclusive charm-production reaction is the quasi-elastic process where a  $d$ -valence quark is changed into a  $c$ -quark, thus transforming the target nucleon into a charmed baryon. Explicitly the quasi-elastic reactions are

$$\nu_\mu n \rightarrow \mu^- \Lambda_c^+ (2285), \quad (13)$$

$$\nu_\mu p \rightarrow \mu^- \Sigma_c^{++} (2455), \quad (14)$$

$$\nu_\mu n \rightarrow \mu^- \Sigma_c^+ (2455), \quad (15)$$

$$\nu_\mu p \rightarrow \mu^- \Sigma_c^{*++} (2520), \quad (16)$$

$$\nu_\mu n \rightarrow \mu^- \Sigma_c^{*+} (2520). \quad (17)$$

In literature there are two classes of models which try to describe the processes (13)-(17). The first class [12]-[17] is based on the  $SU(4)$  flavour symmetry, but since  $SU(4)$  is badly broken, the parameters (axial and vectorial mass) entering the cross-section formula cannot be reliably predicted.

A different approach [18] is based on the Bloom-Gilman [19] local duality in  $\nu N$  scattering modified on the basis of QCD [20, 21].

The cross-sections predicted by the different models, assuming a neutrino energy of 10  $GeV$ , are shown in Table 1. As we can see, these predictions can even differ by one order of magnitude. From Fig. 3 in Refs. [13] and [18] we note that the total cross-section in both models is almost flat for a neutrino energy larger than 8  $GeV$ .

Only one measurement of the neutrino quasi-elastic charm production cross-section exists. The E531 experiment [22], based on a sample of 3 events and

Reaction	$\sigma(10^{-39} \text{ cm}^2)$	$\mathcal{R}(\%)$	Expected events
$\nu_\mu p \rightarrow \mu^- \Sigma_c^{++}$	0.14	0.14	1400
$\nu_\mu p \rightarrow \mu^- \Sigma_c^{*++}$	0.06	0.06	600
$\nu_\mu n \rightarrow \mu^- \Lambda_c^+$	0.3	0.3	3000
$\nu_\mu n \rightarrow \mu^- \Sigma_c^+$	0.07	0.07	700
$\nu_\mu n \rightarrow \mu^- \Sigma_c^{*+}$	0.03	0.03	300
All	0.6	0.6	6000

Table 2: Quasi-elastic charm production cross-section and its contribution to the total charged-current neutrino cross-section. In the last column the expected number of events, assuming a starting sample of 1 million charge-current neutrino-induced events, is shown.

using a neutrino beam with an average energy of  $\sim 22 \text{ GeV}$ , measured the  $\Lambda_c^+$  quasi-elastic production cross-section to be:

$$\sigma(\nu_\mu n \rightarrow \mu^- \Lambda_c^+) = 0.37_{-0.23}^{+0.37} \times 10^{-39} \text{ cm}^2$$

$$\mathcal{R} \equiv \frac{\sigma(\nu_\mu n \rightarrow \mu^- \Lambda_c^+)}{\sigma(\nu_\mu N \rightarrow \mu^- X)} = 0.3_{-0.2}^{+0.3}\%$$

Despite the large statistical error, this measurement is clearly inconsistent with the predictions of Refs. [13]-[16], while the agreement is fair for [12, 17, 18]. An average value of the cross-sections predicted by Refs. [12, 17, 18] has been used to have a rough estimate of the expected number of events, see Table 2.

### 3.2 Topology of the quasi-elastic events

In the quasi-elastic processes (13)-(17), besides the charmed baryon, only a muon is produced at the interaction point (primary vertex). For reaction (13) we expect the topology shown in Fig. 1a), namely, a muon track plus the  $\Lambda_c^+$  immediately decaying. For reactions (14) and (16), since the produced  $\Sigma_c^{++}$  strongly decays into a  $\Lambda_c^+$  and a  $\pi$ , we expect three charged particles at the primary vertex as shown in Fig. 1c). For reactions (15) and (17) we expect a number of charged particles produced at the primary vertex equal to the one of reaction (13), plus a neutral pion produced in the  $\Sigma_c^+$  decay (see Fig. 1b)).

Indeed, these events are characterised by a peculiar topology: two charged tracks produced at the primary vertex, with  $\Sigma_c$ , if present, decaying strongly. In any case, the final charmed baryon can only be a  $\Lambda_c^+$ . This feature is very important and will be exploited heavily in the following.

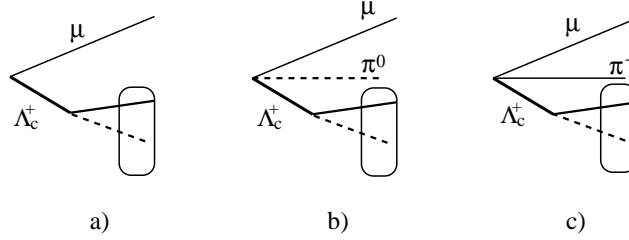


Figure 1: Topology of the quasi-elastic charm neutrino induced events in the case of the reaction a)  $\nu_\mu n \rightarrow \mu^- \Lambda_c^+$ , b)  $\nu_\mu n \rightarrow \mu^- \Sigma_c^+(\Sigma_c^{*+})$  and c)  $\nu_\mu p \rightarrow \mu^- \Sigma_c^{++}(\Sigma_c^{*++})$ . The particles inside the ellipse represent the  $\Lambda_c^+$  decay products.

### 3.3 Kinematics of the quasi-elastic reaction

Let us assume, for simplicity, the initial nucleon at rest. In this frame, given the transferred 4-momentum squared  $q^2$ , the energy of the charmed baryon is

$$E_C = \frac{q^2 + m_C^2 + m_N^2}{2m_N}, \quad (18)$$

where  $m_C$  is its mass and  $m_N$  is the mass of the struck nucleon. The  $q^2$ -distribution, at a fixed neutrino energy,  $(1/\sigma)d\sigma/dq^2$  is in general model dependent [12]-[18]. Nevertheless, despite the large disagreement in the theoretical total cross-sections, the predicted  $q^2$ -distributions are very similar and lie mostly in the range  $0 < q^2 < 2 \text{ GeV}^2$ . We study the kinematics of the quasi-elastic process at different values of  $q^2$  integrating over the neutrino energy spectrum<sup>2</sup>. As reference values of  $q^2$  we use (0.1, 0.5, 1, 2)  $\text{GeV}^2$ .

The flight length and the decay kinematics of the  $\Lambda_c^+$  have been evaluated using the package PYTHIA5.7/JETSET7.4 [24]. The flight length distributions for four different  $q^2$  values are shown in Fig. 2. From this figure we can see that, because of the small  $\gamma$  factor, almost all the  $\Lambda_c^+$  decay within 500  $\mu\text{m}$  from the production point. This parameter is crucial when we start thinking of a detector able to *see* the topologies shown in Fig. 1.

### 3.4 Deep inelastic charm processes

Charmed hadrons can be produced in deep inelastic neutrino interactions through the reaction  $\nu_\mu N \rightarrow \mu^- CX$ , where  $C = D^0, D^+, D_s^+, \Lambda_c^+$  and  $X$  is purely hadronic. Using the CERN-SPS WANF neutrino beam [23], (57±5)% of the charmed particles produced in deep inelastic interactions is neutral. The rest can be split as follows: (19±4)%  $D^+$ , (12±4)%  $D_s^+$  and (12±3)%  $\Lambda_c^+$ . For details about the charm production fractions in neutrino interactions we refer

<sup>2</sup>As an example of neutrino beam we considered the CERN-SPS WANF neutrino beam [23], which has an average energy of about of 27  $\text{GeV}$ .

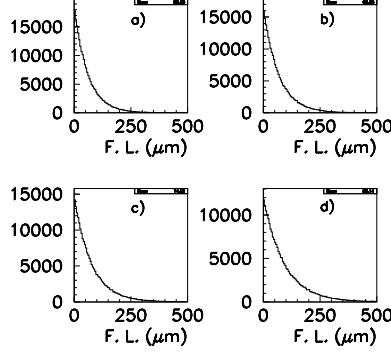


Figure 2: Flight length distribution for different  $q^2$  values: a)  $q^2 = 0.1 \text{ GeV}^2$ , b)  $q^2 = 0.5 \text{ GeV}^2$ , c)  $q^2 = 1 \text{ GeV}^2$ , d)  $q^2 = 2 \text{ GeV}^2$ .

to [25].

Through a Monte Carlo simulation, we also checked that  $(15.48 \pm 0.09)\%$  of the deep inelastic events with a charmed hadron in the final state has a topology similar to those shown in Fig. 1a) and Fig. 1b) and  $(8.43 \pm 0.04)\%$  to the one in Fig. 1c).

### 3.5 Quasi-elastic versus deep inelastic charm events

A suitable variable to discriminate quasi-elastic from deep inelastic events is the visible hadronic energy, see Fig. 3. According to Eq. (18), a large fraction of the visible energy in quasi-elastic events is expected to lie in the range  $(3 \div 5) \text{ GeV}$ . It is, indeed, possible to achieve a high rejection power against deep inelastic events keeping high efficiency for quasi-elastic ones. For example, the cut  $E_{vis} \leq 5 \text{ GeV}$  rejects  $(97.1 \pm 0.1)\%$  of the deep inelastic processes keeping more than 90% of quasi-elastic events.

It is important to have high rejection power against deep inelastic charm production due to its large cross-section [22] ( $\sigma(\nu_\mu N \rightarrow \mu^- CX)/\sigma(\nu_\mu N \rightarrow \mu^- X) \sim 5\%^3$ ,  $\mathcal{R} = 0.6\%$ ) and to the fact that not only  $\Lambda_c^+$ , but also  $D^+$  and  $D_s^+$  are produced. In fact,  $D^+$  or  $D_s^+$  hadrons, wrongly identified, could bias the determination of the  $\Lambda_c^+$  branching ratios. The quasi-elastic sample contamination, which comes from deep inelastic events, can be written using Table 1 as

$$\varepsilon_{fake} = \frac{\sigma(\nu_\mu N \rightarrow \mu^- CX)}{\sigma(\nu_\mu N \rightarrow \mu^- X)} \times \frac{1}{\mathcal{R}} \times f_{fake} \times f_{E < 5 \text{ GeV}} \times f_{(D^+ \text{ or } D_s^+)} \quad (19)$$

<sup>3</sup>This result includes also the production of neutral charmed particles.

$\Delta\mathcal{R}/\mathcal{R}$	$\sigma_{fake}/\varepsilon_{fake}$	$\varepsilon_{fake}$
10%	19%	$(0.45\pm0.09)\%$
30%	34%	$(0.45\pm0.15)\%$
50%	53%	$(0.45\pm0.24)\%$
100%	101%	$(0.45\pm0.45)\%$
200%	201%	$(0.45\pm0.90)\%$
500%	500%	$(0.45\pm2.25)\%$

Table 3: The relative and absolute errors on  $\varepsilon_{fake}$  are shown as a function of the relative error on  $\mathcal{R}$ .

The factor  $f_{fake}(= (23.9\pm0.1)\%)$  denotes the fraction of deep inelastic events which fakes a quasi-elastic topology,  $f_{E<5GeV}(= (2.9\pm0.1)\%)$  is the fraction of the deep inelastic events which survives to the energy cut, and  $f_{(D^+orD_s^+)}(= (8.2\pm0.4)\%)$  is the fraction, among *fake* quasi-elastic, with a charmed meson in the final state. Hence, the contamination is  $\varepsilon_{fake} \simeq 0.5\%$ . The relative error on  $\varepsilon_{fake}$  as a function of the relative error on  $\mathcal{R}$  is shown in Table 3.

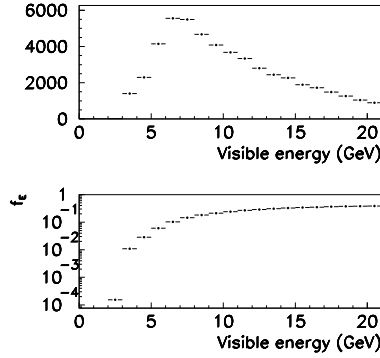


Figure 3: Top: Visible energy distribution of deep inelastic charm events with a vertex topology similar to the one shown in Fig. 1a) and Fig. 1b). Bottom: fraction of deep inelastic charm events faking a quasi-elastic topology as a function of the energy cut.

## 4 Description of the method

Due to the peculiar topology and kinematics of the quasi-elastic events an almost pure sample of  $\Lambda_c^+$ , with a small contamination of  $D^+$  and  $D_s^+$  produced in deep



inelastic events, can be selected. No model dependent information is used to determine the number of  $\Lambda_c^+$ . The contamination of  $D^+$  and  $D_s^+$  from deep inelastic events can be taken into account assigning it as relative systematic error on the branching ratios. We assumed the relative systematic error to be  $\varepsilon_{fake} + 3\sigma_{fake}$ . The normalisation to determine the  $\Lambda_c^+$  absolute branching ratios is simply given by the number of events with a vertex topology consistent with Fig. 1. We want to stress, here, that no model dependent information is used to determine the normalisation. The little knowledge we have about the quasi-elastic charm production cross-section, which is model dependent unless measured, plays a role only in the evaluation of the deep inelastic contamination, namely the systematic error. It is worth noticing that, even if the ratio  $\mathcal{R}$  is known with an uncertainty of 500%<sup>4</sup>, the relative systematic error on the branching ratios is  $\sim 7.2\%$  (see Table 3).

#### 4.1 Measurement accuracy in a *perfect detector*

The *perfect detector* by definition has the following features:

- vertex topology measurement with 100% efficiency resolution for charmed baryon decays;
- infinite energy resolution;
- particle identification capability with infinite resolution.

In Table 4 the expected accuracy on the determination of the  $\Lambda_c^+$  branching ratios as a function of the relative error on  $\mathcal{R}$  is shown. To compute the expected number of events in each decay channel we used the central values (shown in Table 4 together with their errors) given by the Particle Data Group [1]. From this Table we can see that, even assuming very large (unrealistic) systematic error, it is still possible to discriminate among methods  $\mathcal{A}$  and  $\mathcal{B}$  discussed in Section 2. In Table 5 the achievable accuracy on the absolute  $BR$  determination as a function of the collected charged-current statistics is shown.

#### 4.2 Measurement accuracy with statistics of present and future experiments

Among the neutrino experiments which are currently taking data or analysing data, CHORUS [26], which uses nuclear emulsions as a target, has an adequate spatial resolution to fully exploit the topologies shown in Fig. 1. Starting from a sample of about of 500000 charged-current events, it is estimated that  $\sim 350000$  events will be analysed in the emulsions [27]. Assuming a 50% efficiency to detect the  $\Lambda_c^+$  decay and taking into account that  $\mathcal{R} = 0.6\%$ , a statistics of  $\sim 1000$  quasi-elastic events can be expected. Due to the good muon identification of the electronic detector and the emulsion capability in identifying electrons,

---

<sup>4</sup>Nevertheless, this is not the case. We recall that E531 [22], with only 3 events observed, measured  $\mathcal{R}$  with an accuracy of 100%.

Channel	PDG BR [1]	$\Delta BR$ ( $\frac{\Delta \mathcal{R}}{\mathcal{R}} = 10\%$ )	$\Delta BR$ ( $\frac{\Delta \mathcal{R}}{\mathcal{R}} = 100\%$ )	$\Delta BR$ ( $\frac{\Delta \mathcal{R}}{\mathcal{R}} = 500\%$ )
$\Lambda_c^+ \rightarrow pK^0$	$(2.5 \pm 0.7)\%$	$(\pm 0.2 \pm 0.02)\%$	$(\pm 0.2 \pm 0.05)\%$	$(\pm 0.2 \pm 0.2)\%$
$\Lambda_c^+ \rightarrow pK^-\pi^+$	$(5.0 \pm 1.3)\%$	$(\pm 0.3 \pm 0.04)\%$	$(\pm 0.3 \pm 0.09)\%$	$(\pm 0.3 \pm 0.4)\%$
$\Lambda_c^+ \rightarrow pK^0\eta$	$(1.3 \pm 0.4)\%$	$(\pm 0.1 \pm 0.01)\%$	$(\pm 0.1 \pm 0.02)\%$	$(\pm 0.1 \pm 0.09)\%$
$\Lambda_c^+ \rightarrow pK^0\pi^+\pi^-$	$(2.4 \pm 1.1)\%$	$(\pm 0.2 \pm 0.02)\%$	$(\pm 0.2 \pm 0.04)\%$	$(\pm 0.2 \pm 0.2)\%$
$\Lambda_c^+ \rightarrow pK^-\pi^+\pi^0$	$(4.7 \pm 1.3)\%$	$(\pm 0.3 \pm 0.04)\%$	$(\pm 0.3 \pm 0.08)\%$	$(\pm 0.3 \pm 0.3)\%$
$\Lambda_c^+ \rightarrow \Lambda\pi^+\pi^0$	$(3.6 \pm 1.3)\%$	$(\pm 0.2 \pm 0.03)\%$	$(\pm 0.2 \pm 0.06)\%$	$(\pm 0.2 \pm 0.3)\%$
$\Lambda_c^+ \rightarrow \Lambda\pi^+\pi^+\pi^-$	$(3.3 \pm 1.0)\%$	$(\pm 0.2 \pm 0.02)\%$	$(\pm 0.2 \pm 0.06)\%$	$(\pm 0.2 \pm 0.2)\%$
$\Lambda_c^+ \rightarrow \Lambda\pi^+\eta$	$(1.7 \pm 0.6)\%$	$(\pm 0.2 \pm 0.01)\%$	$(\pm 0.2 \pm 0.03)\%$	$(\pm 0.2 \pm 0.1)\%$
$\Lambda_c^+ \rightarrow \Sigma^+\pi^0$	$(1.0 \pm 0.3)\%$	$(\pm 0.1 \pm 0.01)\%$	$(\pm 0.1 \pm 0.02)\%$	$(\pm 0.1 \pm 0.07)\%$
$\Lambda_c^+ \rightarrow \Sigma^+\pi^+\pi^-$	$(3.4 \pm 1.0)\%$	$(\pm 0.2 \pm 0.02)\%$	$(\pm 0.2 \pm 0.06)\%$	$(\pm 0.2 \pm 0.2)\%$
$\Lambda_c^+ \rightarrow \Sigma^-\pi^+\pi^+$	$(1.8 \pm 0.8)\%$	$(\pm 0.2 \pm 0.01)\%$	$(\pm 0.2 \pm 0.03)\%$	$(\pm 0.2 \pm 0.1)\%$
$\Lambda_c^+ \rightarrow \Sigma^0\pi^+\pi^0$	$(1.8 \pm 0.8)\%$	$(\pm 0.2 \pm 0.01)\%$	$(\pm 0.2 \pm 0.03)\%$	$(\pm 0.2 \pm 0.1)\%$
$\Lambda_c^+ \rightarrow \Sigma^0\pi^+\pi^+\pi^-$	$(1.1 \pm 0.4)\%$	$(\pm 0.1 \pm 0.01)\%$	$(\pm 0.1 \pm 0.02)\%$	$(\pm 0.1 \pm 0.08)\%$
$\Lambda_c^+ \rightarrow \Sigma^+\pi^+\pi^-\pi^0$	$(2.7 \pm 1.0)\%$	$(\pm 0.2 \pm 0.02)\%$	$(\pm 0.2 \pm 0.05)\%$	$(\pm 0.2 \pm 0.2)\%$
$\Lambda_c^+ \rightarrow \Lambda\mu^+\nu_\mu$	$(2.0 \pm 0.7)\%$	$(\pm 0.2 \pm 0.01)\%$	$(\pm 0.2 \pm 0.04)\%$	$(\pm 0.2 \pm 0.1)\%$
$\Lambda_c^+ \rightarrow \Lambda e^+\nu_e$	$(2.1 \pm 0.7)\%$	$(\pm 0.2 \pm 0.01)\%$	$(\pm 0.2 \pm 0.04)\%$	$(\pm 0.2 \pm 0.2)\%$

Table 4: Statistical and systematic accuracy achievable in the determination of the  $\Lambda_c^+$  absolute branching ratios, assuming a collected statistics of  $10^6$   $\nu_\mu$  charged-current events, as a function of the relative error on  $\mathcal{R}$ . The central values are taken from ref. [1].

Channel	$N_\mu = 10^6$	$N_\mu = 10^5$	$N_\mu = 10^4$
$\Lambda_c^+ \rightarrow pK^0$	$(\pm 0.2 \pm 0.05)\%$	$(\pm 0.6 \pm 0.05)\%$	$(\pm 1.8 \pm 0.05)\%$
$\Lambda_c^+ \rightarrow pK^-\pi^+$	$(\pm 0.3 \pm 0.09)\%$	$(\pm 0.9 \pm 0.09)\%$	$(\pm 2.8 \pm 0.09)\%$
$\Lambda_c^+ \rightarrow pK^0\eta$	$(\pm 0.1 \pm 0.02)\%$	$(\pm 0.5 \pm 0.02)\%$	$(\pm 1.7 \pm 0.02)\%$
$\Lambda_c^+ \rightarrow pK^0\pi^+\pi^-$	$(\pm 0.2 \pm 0.04)\%$	$(\pm 0.6 \pm 0.04)\%$	$(\pm 1.0 \pm 0.04)\%$
$\Lambda_c^+ \rightarrow pK^-\pi^+\pi^0$	$(\pm 0.3 \pm 0.08)\%$	$(\pm 0.9 \pm 0.08)\%$	$(\pm 2.8 \pm 0.08)\%$
$\Lambda_c^+ \rightarrow \Lambda\pi^+\pi^0$	$(\pm 0.2 \pm 0.06)\%$	$(\pm 0.8 \pm 0.06)\%$	$(\pm 2.3 \pm 0.06)\%$
$\Lambda_c^+ \rightarrow \Lambda\pi^+\pi^+\pi^-$	$(\pm 0.2 \pm 0.06)\%$	$(\pm 0.7 \pm 0.06)\%$	$(\pm 2.3 \pm 0.06)\%$
$\Lambda_c^+ \rightarrow \Lambda\pi^+\eta$	$(\pm 0.2 \pm 0.03)\%$	$(\pm 0.5 \pm 0.03)\%$	$(\pm 1.7 \pm 0.03)\%$
$\Lambda_c^+ \rightarrow \Sigma^+\pi^0$	$(\pm 0.1 \pm 0.02)\%$	$(\pm 0.4 \pm 0.02)\%$	$(\pm 1.0 \pm 0.02)\%$
$\Lambda_c^+ \rightarrow \Sigma^+\pi^+\pi^-$	$(\pm 0.2 \pm 0.06)\%$	$(\pm 0.7 \pm 0.06)\%$	$(\pm 2.3 \pm 0.06)\%$
$\Lambda_c^+ \rightarrow \Sigma^-\pi^+\pi^+$	$(\pm 0.2 \pm 0.03)\%$	$(\pm 0.5 \pm 0.03)\%$	$(\pm 1.7 \pm 0.03)\%$
$\Lambda_c^+ \rightarrow \Sigma^0\pi^+\pi^0$	$(\pm 0.2 \pm 0.03)\%$	$(\pm 0.5 \pm 0.03)\%$	$(\pm 1.7 \pm 0.03)\%$
$\Lambda_c^+ \rightarrow \Sigma^0\pi^+\pi^+\pi^-$	$(\pm 0.1 \pm 0.02)\%$	$(\pm 0.4 \pm 0.02)\%$	$(\pm 1.0 \pm 0.02)\%$
$\Lambda_c^+ \rightarrow \Sigma^+\pi^+\pi^-\pi^0$	$(\pm 0.2 \pm 0.05)\%$	$(\pm 0.7 \pm 0.05)\%$	$(\pm 2.2 \pm 0.05)\%$
$\Lambda_c^+ \rightarrow \Lambda\mu^+\nu_\mu$	$(\pm 0.2 \pm 0.04)\%$	$(\pm 0.6 \pm 0.04)\%$	$(\pm 1.8 \pm 0.04)\%$
$\Lambda_c^+ \rightarrow \Lambda e^+\nu_e$	$(\pm 0.2 \pm 0.04)\%$	$(\pm 0.6 \pm 0.04)\%$	$(\pm 1.8 \pm 0.04)\%$

Table 5: Accuracy achievable ( $\Delta BR$ ), assuming a 100% error on  $\mathcal{R}$ , as a function of the collected charged-current statistics.

CHORUS is well suited to study  $\Lambda_c^+$  semi-leptonic decays. Assuming 100% error on  $\mathcal{R}$  and the PDG central value [1], the following accuracy could be achieved:

$$\Delta BR(\Lambda_c^+ \rightarrow \Lambda \mu^+ \nu_\mu) = (\pm 0.44 \text{ }_{stat} \pm 0.01 \text{ }_{sys})\% \quad (20)$$

$$\Delta BR(\Lambda_c^+ \rightarrow \Lambda e^+ \nu_e) = (\pm 0.45 \text{ }_{stat} \pm 0.01 \text{ }_{sys})\% \quad (21)$$

A measurement with higher sensitivity could be performed exposing a dedicated detector, whose feasibility study has not yet been worked out, at the future neutrino beams from muon storage rings [28]. Such beams could provide  $\mathcal{O}(10^6)$   $\nu_\mu - CC$  events/year in a 10 kg fiducial mass detector, 1 km away from the neutrino source, allowing for a strong reduction of the statistical uncertainty on the  $\Lambda_c$  branching ratios, see Table 5.

## Conclusions

We have presented a new method for a direct evaluation of the  $\Lambda_c^+$  branching ratios. We have also stressed that this has very interesting consequences for our understanding of baryon production in charm decays. Even just a good determination of the  $\Lambda_c^+$  semi-leptonic exclusive decay widths would be sufficient: indeed from Eq.(4) we would determine  $BR(\Lambda_c^+ \rightarrow p K^- \pi^+)$ , very important phenomenologically as pointed out particularly in Section 2. We have also shown that, already with existing data, it should be possible to perform a direct measurement of  $\Lambda_c^+$  exclusive decay widths, which is lacking to date.

## References

- [1] Particle Data Group, Euro. Phys. J. 1 (1998) 1.
- [2] I. Dunietz, Phys. Rev. D 58 (1998) 094010.
- [3] H. Albrecht et al., ARGUS Collaboration, Phys. Lett. B 207 (1988) 109.
- [4] G. Crawford et al., CLEO Collaboration, Phys. Rev. D 45 (1992) 752.
- [5] H. Albrecht et al., ARGUS Collaboration, Z. Phys. C 56 (1992) 1.
- [6] H. Albrecht et al., ARGUS Collaboration, Phys. Rept. 276 (1996) 223.
- [7] P. Avery et al., CLEO Collaboration, Phys. Rev. D 43 (1991) 3599.
- [8] H. Albrecht et al., ARGUS Collaboration, Phys. Lett. B 269 (1991) 134.
- [9] T. Bergfeld et al., CLEO Collaboration, Phys. Lett. B 323 (1994) 219.
- [10] A. Bean et al., CLEO Collaboration, Phys. Lett. B 317 (1993) 647.
- [11] J. Chay, H. Georgi, B. Grinstein, Phys. Lett. B 247 (1990) 399; I.I. Bigi, N.G. Uraltsev, A.I. Vainshtein, Phys. Lett. B 293 (1992) 430, Erratum Phys. Lett. B 297 (1993) 477; A. Manohar and M.B. Wise, Phys. Rev. D 49(1994) 1310; I.I. Bigi, hep-ph/9508408;
- [12] J. Finjord and F. Ravndal, Phys. Lett. B 58 (1975) 61.
- [13] R.E. Shrock and B.W. Lee, Phys. Rev. D 13 (1976) 2539.

- [14] C. Avilez et al., Phys. Lett. B 66 (1977) 149.
- [15] C. Avilez and T. Kobayashi, Phys. Rev. D 19 (1979) 3448.
- [16] C. Avilez et al., Phys. Rev. D 17 (1978) 709.
- [17] A. Amer et al., Phys. Lett. B 81 (1979) 48.
- [18] S.G. Kovalenko, Sov. J. Nucl. Phys. 52 (1990) 934.
- [19] E.D. Bloom and F.G. Gilman, Phys. Rev. D 4 (1971) 2901.
- [20] A. De Rújula et al., Ann. Phys. 103 (1977) 315.
- [21] A. De Rújula et al., Phys. Rev. D 15 (1977) 2415.
- [22] N. Ushida et al., E531 Collaboration, Phys. Lett. B 206 (1988) 375.
- [23] G. Acquistapace et al., CERN Preprint, CERN-ECP/95-14, 1995.
- [24] T. Sjöstrand, Comp. Phys. Comm. 82 (1994) 74.
- [25] T. Bolton, hep-ex/9708014.
- [26] E. Eskut et al., Nucl. Instr. Meth. A 401 (1998) 7.
- [27] E. Eskut et al., Phys. Lett. B 424 (1998) 202; E. Eskut et al., Phys. Lett. B 434 (1998) 205.
- [28] S. Geer, Phys. Rev. D 57 (1998) 1.